

# Thermal response of epitaxial thin Bi films on Si(001) upon femtosecond laser excitation studied by ultrafast electron diffraction

A. Hanisch, B. Krenzer,\* T. Pelka, S. Möllenbeck, and M. Horn-von Hoegen

Center for Nanointegration (CeNIDE), Department of Physics, University of Duisburg-Essen, Lotharstrasse 1, 47048 Duisburg, Germany

(Received 30 November 2007; revised manuscript received 7 February 2008; published 13 March 2008)

The thermal response of epitaxial Bi films deposited on Si(001) upon femtosecond laser pulse excitation is investigated by means of ultrafast electron diffraction. The initial surface temperature increase is caused by linear absorption of 800 nm photons. The exponential decay of the transient film temperature is governed by the thermal boundary conductance of the Bi-Si interface. The decay constant linearly depends on the film thickness and was found between 550 and 1100 ps in the thickness range from 6 to 12.2 nm. The thermal boundary conductance of the Bi-Si interface extracted from the linear dependence yields  $\sigma_K = (1320 \pm 60) \text{ W}/(\text{cm}^2 \text{ K})$  in accordance with earlier calculations.

DOI: 10.1103/PhysRevB.77.125410

PACS number(s): 61.05.jh, 44.10.+i, 68.35.-p

## INTRODUCTION

Compared to heat transport in homogeneous materials, the thermal transport properties of composite systems are drastically altered.<sup>1-4</sup> Any interface between two different materials acts as a barrier to thermal heat diffusion, decreasing the thermal diffusivity by orders of magnitude.<sup>5,6</sup> For thin films deposited on a substrate, the temporal evolution of the film temperature subsequent to thermal excitation is described by

$$cd \frac{\partial T(t)}{\partial t} = -\sigma_K (T_f(t) - T_s(t)), \quad (1)$$

where  $c$  is the specific heat capacity and  $d$  the film thickness.<sup>4</sup>  $\sigma_K$  is the thermal boundary conductance that relates the heat flux across the interface to the temperature difference ( $T_f - T_s$ ) at the interface, where  $T_f$  and  $T_s$  are the film and substrate temperatures.<sup>2-4</sup> For a constant substrate temperature  $T_s$ , Eq. (1) results in an exponential decay with a time constant as follows:<sup>4,7</sup>

$$\tau = \frac{c}{\sigma_K} d. \quad (2)$$

By assuming that the heat transport across the interface is only mediated by phonons, the thermal boundary conductance can be written as<sup>2,8</sup>

$$\sigma_K = \frac{1}{2} \int_0^\infty c(\omega, T) \langle v_z(\omega) \rangle \langle t(\omega) \rangle d\omega, \quad (3)$$

where  $c(\omega, T)$  is the specific heat capacity of phonons of frequency  $\omega$ .  $\langle v_z(\omega) \rangle$  and  $\langle t(\omega) \rangle$  are the average phonon velocity perpendicular to the interface and phonon transmission probability, respectively. The fundamental physical assumption in deriving Eq. (3) is that only a fraction of the energy carried by phonons is transported across the interface. In order to get a microscopic picture of the heat transport across the interface, one has to develop models for the calculation of the phonon transmission probability, which has been carried out by a large number of authors in the past.<sup>3,4,8-15</sup> Basically, two different regimes are distinguished.<sup>9</sup> If the dominant phonon wavelength is larger than the interface

roughness, the phonons can be treated as elastic waves (acoustic mismatch model). The transmission probability is given by the ratio of the energy carried by the refracted waves to the energy carried by the incident wave.<sup>3,4,16</sup> Using the transmission probabilities calculated on the basis of this model yields thermal boundary conductances that are in good agreement with experimental values obtained at sufficiently low temperatures ( $T_f < 30 \text{ K}$ ).<sup>3</sup>

In the second regime for dominant phonon wavelengths that are smaller than the interface roughness, strong elastic scattering at the interface is assumed (diffusive mismatch model). In this case, the phonon transmission probability is given by the density of states in the two adjacent media.<sup>3,4</sup> For solid-solid interfaces and by using the Debye approximation, this model results in comparable thermal boundary resistances as in the first case. For higher temperatures, however, both models fail to describe the observed thermal boundary conductances, which was attributed to additional effects not included in the above models, e.g., inelastic scattering or interface roughening. This led Cahill *et al.*<sup>2</sup> to the conclusion that the microscopic picture of the heat transport at an interface is not complete. By reviewing the literature, it can also be concluded that the discrepancies between theory and experiment are caused by unknown interface properties that result in more complex energy transfer processes at the interface.<sup>17</sup> From the experimental point of view, this requires studies of model systems exhibiting well defined and well characterized interfaces.

Such model systems are thin bismuth films grown on single crystalline silicon substrates. Bi grows epitaxially in a defined crystallographic orientation on a Si(001) surface.<sup>18-20</sup> Additionally, as no Bi-silicide formation or Bi diffusion into Si is known, the Bi-Si interface can be considered abrupt. For the growth of Bi on the Si(111) surface, an atomically well defined, abrupt interface has been observed experimentally.<sup>21</sup> In previous studies, we investigated the thermal response of a 5.5 nm thin Bi film by means of ultrafast electron diffraction.<sup>22,23</sup> We found good agreement between the measured thermal boundary conductance and the value obtained by using the phonon transmission probability calculated in the two above described models.

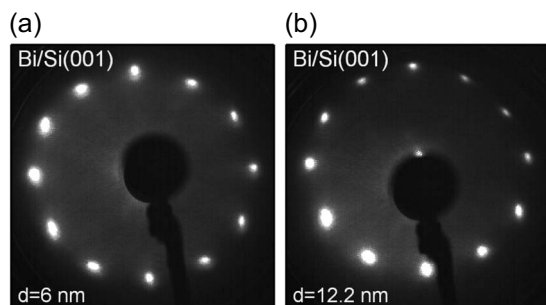


FIG. 1. LEED patterns of Bi films on Si(001) with (a) 6 nm and (b) 12.2 nm thicknesses. The electron energy was set to 92 eV for both images. The 12-fold pattern is caused by the incoherent superposition of two hexagonal LEED patterns rotated by  $90^\circ$ . The somewhat elongated spots in (a) and (b) have their origin in the formation of an ordered dislocation array, resulting in a periodic height undulation of the surface. With increasing film thickness, the surface undulation decreases, resulting in more circular diffraction spots (Refs. 18 and 19). The nonuniform intensity distribution of the diffraction spots along the 12-fold ring is due to the experimental setup.

This paper extends these studies by investigating the dependence of the surface temperature evolution on pump fluence and film thickness. It will be shown that the heating of the film is a result of linear absorption and that the surface temperature decay constant linearly depends on the film thickness as expected from Eq. (2). A great advantage of this study is the *in situ* preparation of the thin Bi films under the cleanest conditions, reducing the number of unknown parameters affecting the interface structure to a minimum. Additionally, very thin films with a controlled thickness have been prepared.

## EXPERIMENT

The Bi films were prepared in the same ultrahigh vacuum system ( $p_{\text{Base}} < 2 \times 10^{-10}$  mbar) as the experiments by depositing high purity Bi (99.9999%, MaTeK) from a Knudsen cell<sup>24</sup> onto a Si(001) surface at room temperature. During deposition, the pressure stayed below  $2 \times 10^{-9}$  mbar. Prior to the Bi deposition, the Si substrate was flashed to  $\sim 1500$  K, resulting in a well ordered ( $2 \times 1$ )-reconstructed surface at 300 K, which was checked by low energy electron diffraction (LEED). Under these conditions, Bi epitaxially grows in the (111) direction.<sup>19,20</sup> Different film thicknesses were prepared either by direct deposition of the desired amount or by consecutive deposition of bismuth. The amount of deposited material was monitored using a quartz microbalance. For calibration the thickness of one film was determined *ex situ* by atomic force microscopy (AFM) and x-ray reflectometry. After each deposition, the film quality was checked by LEED. The diffraction patterns of films with thicknesses of 6 and 12.2 nm, which are the thinnest and thickest films investigated in this study, are shown in Fig. 1.

The 12-fold symmetry of the patterns is caused by the incoherent superposition of two hexagonal LEED patterns of Bi(111) crystallites rotated by  $90^\circ$ . The diffraction pattern of

the 6 nm thin Bi film [Fig. 1(a)] shows somewhat elongated spots, which are caused by the formation of an ordered dislocation network resulting in a periodic height undulation of the surface.<sup>18,19</sup> For thicker films, the surface height undulation vanishes and the diffraction spots appear much more symmetric for the 12.2 nm film shown in Fig. 1(b).<sup>20</sup> The nonuniform intensity distribution along the 12-fold ring is caused by the experimental setup. The LEED patterns of films with thicknesses below 10 nm and electron energies larger than 140 eV show very weak remains of Si(001)( $2 \times 1$ ) diffraction spots, which is indicative of the existence of a few pinholes in the Bi film.

The transient temperature evolution of the thin films was determined by means of ultrafast electron diffraction at surfaces.<sup>22,23,25</sup> Briefly, a short electron pulse is diffracted at a surface for different delays from an initial short laser pulse excitation. Because of the Debye-Waller effect, the diffraction spot intensity is affected by the surface temperature, which is used to extract the transient temperature evolution.<sup>22,23,25,26</sup> We found that the magnitude of the Debye-Waller effect for a given scattering setup is independent of Bi film thickness, which is explained by a thickness-independent surface Debye temperature  $\theta_D^{\text{surf}}$ . The sample width for all experiments was 2 mm and the base temperature was 80 K, slightly below the Bi Debye temperature of  $\theta_D = 119$  K.<sup>27</sup> Electrons of energy 7 keV were scattered at an angle of incidence of  $5^\circ$ , resulting in a perpendicular momentum transfer of  $\Delta k_\perp = 7.47 \text{ \AA}^{-1}$ . The diffraction patterns were intensified using a microchannel plate detector and recorded by a cooled charge coupled device camera.<sup>26</sup> The sample was excited by  $\sim 50$  fs short laser pulses at a wavelength of 800 nm. The source for the short pulses is a commercial regenerative amplifier (Legend, Coherent) with an output power of 2.3 W at a repetition rate of 5 kHz. The excited area on the sample ( $3 \times 2 \text{ mm}^2$ ) was larger than the probed area ( $0.4 \times 2 \text{ mm}^2$ ).

## DATA ANALYSIS

Figure 2 shows the surface temperature evolution of an 11 nm thin Bi film excited at a fluence of  $Q_A = 2.9 \text{ mJ/cm}^2$ . At zero delay, the surface temperature increases steeply from 80 to 170 K. For larger delays, the surface temperature decays slowly within a few nanoseconds to the base temperature of  $T_0 = 80$  K. The whole temperature evolution can be well described with a phenomenological function that has been used previously in describing the transient reflectivity evolution of laser heated metal surfaces,<sup>28,29</sup>

$$T(t) = \Theta(t) \Delta T (1 - e^{-t/\tau_1}) e^{-t/\tau_2} + T_0, \quad (4)$$

where  $\Theta(t)$  is the Heaviside step function and  $\Delta T$  the initial temperature jump. The delay  $t=0$  denotes the temporal overlap of pump and probe pulses. The first factor in Eq. (4) describes the surface temperature increase with a time constant  $\tau_1$ , the second the decrease with a decay constant  $\tau_2$ . The fit of Eq. (4) to the data is shown in Fig. 2 as a solid line. The fit yields  $\tau_1 = (37 \pm 4)$  ps,  $\tau_2 = (1390 \pm 70)$  ps, and  $\Delta T = (95 \pm 5)$  K.

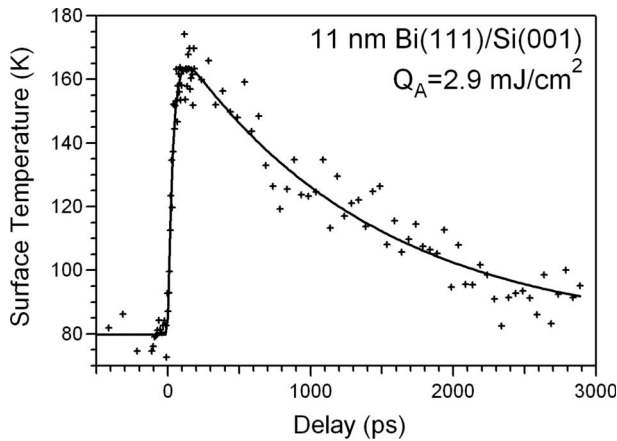


FIG. 2. Surface temperature evolution of an 11 nm thin Bi film deposited on Si(001) at 300 K. The laser fluence is  $Q_A = 2.9 \text{ mJ/cm}^2$ . The solid line is a fit to the data with the function from Eq. (4) described in the text.

The observed temperature increase is a result of the response of the system to the short pulse excitation convoluted with the temporal resolution of the experiment. In the experiment, the temporal resolution is determined by the velocity mismatch between the probing electrons and the excitation.<sup>22</sup> Basically, the time resolution is given by the sampling time of the electron pulse which, in this experiment, is  $\sim 40$  ps. On this time scale, fast responses of the system, e.g., change of structure factor<sup>30</sup> and delayed lattice temperature increase due to electron-phonon coupling, are not resolvable. We attribute the value of  $\tau_1$  to be given by the limited temporal resolution and conclude that the observed change in diffraction spot intensity is due to the change in vibrational energy, i.e., temperature. This attribution is supported by the observation that the value of  $\tau_1$  has always been found between 25 and 40 ps with no obvious dependence on the applied fluence or film thickness.

The decay constant  $\tau_2$ , however, is connected to the thermal boundary conductance  $\sigma_K$  [cf. Eq. (2)]. Because of the orders of magnitude smaller absorption coefficient and higher heat diffusion constant of Si compared to Bi, the assumption of a constant Si substrate temperature is fulfilled and Eq. (2) can be applied.<sup>7,22,23</sup> Moreover, due to heat diffusion in the film, a homogeneous temperature distribution across the film is established after  $\sim 10$  ps and the surface temperature displays the temperature of the thin film.<sup>7</sup> Compared to our previous approach in obtaining the thermal boundary conduction by fitting the decay with a single exponential function,<sup>22,23</sup> the fits of Eq. (4) to the experimental data yield the same results, within the error.

### INITIAL TEMPERATURE INCREASE $\Delta T$

In Fig. 3, the dependence of the initial temperature increase  $\Delta T$  defined by Eq. (4) on the applied fluence  $Q_A$  and Bi film thickness is shown. Figure 3(a) shows a linear relationship between  $\Delta T$  and the fluence. For the investigated 11 nm thin Bi film, the linear fit yields a slope of

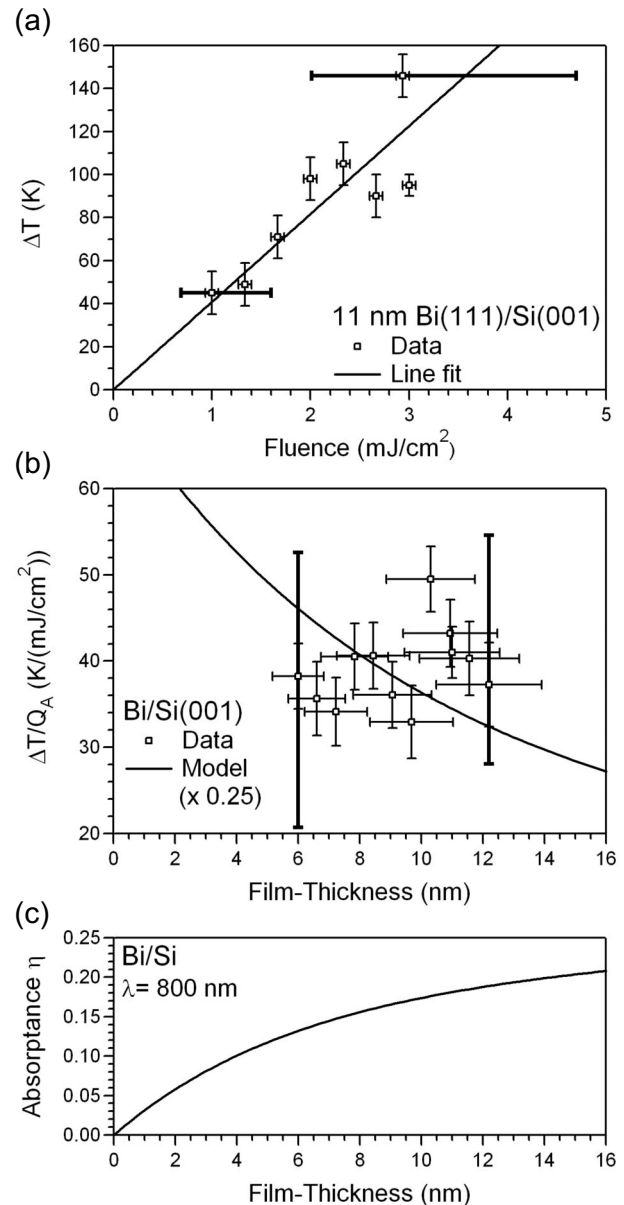


FIG. 3. Dependence of the initial temperature increase  $\Delta T$  on (a) the fluence  $Q_A$  for an 11 nm thin Bi film and (b) the film thickness. The larger error bars in (a) and (b) represent the systematic error in the determination of the pumped area, the smaller error bars the error obtained from the fit of Eq. (4). The slope of the line fit in (a) is  $(41 \pm 3) \text{ K}/(\text{mJ}/\text{cm}^2)$ . The line in (b) is obtained from a simple model described in the text. (c) Absorbance  $\eta$  of the Bi film for  $\lambda = 800 \text{ nm}$  obtained from multilayer optics using the optical constants from Table I.

$(41 \pm 3) \text{ K}/(\text{mJ}/\text{cm}^2)$ . Because of the systematic error in the determination of the pumped area with an accuracy of 0.5 mm, this slope lies between 26 and 60  $\text{K}/(\text{mJ}/\text{cm}^2)$ . The observed linear relationship between initial temperature rise and fluence has been verified for two additional films with different thicknesses. Because of this linear relationship, it is sufficient to determine  $\Delta T/Q_A$  for only one fluence. The variation of  $\Delta T/Q_A$  for Bi film thicknesses in the range between 6 and 12.2 nm is shown in Fig. 3(b). As evident from

TABLE I. Bulk values for the specific heat capacity  $c$ , index of refraction  $n$ , extinction coefficient  $\kappa$ , reflectivity  $r$ , and mean absorption depth  $\alpha^{-1}$  for light of wavelength 800 nm of bismuth and silicon at 300 K (Refs. 34–36).

	$c[10^6 \text{ J}/(\text{K m}^3)]$	$n$	$\kappa$	$r$	$\alpha^{-1}(\text{nm})$
Bi	1.19	2.75	4.27	0.66	14.9
Si	1.68	3.673	0.005	0.33	12732

Fig. 3(b),  $\Delta T/Q_A$  is almost constant, only slightly increasing with film thickness.

Assuming homogeneous heating across a film of thickness  $d$  and linear absorption, the slope can be estimated by

$$\frac{\Delta T}{Q_A} = \frac{\eta(d)}{cd}, \quad (5)$$

where  $c$  denotes the specific heat capacity.  $\eta(d)$  is the thickness-dependent absorptance of the thin film, with  $\eta(d) = 1 - r(d) - t(d)$ . The effective reflectance  $r(d)$  and transmittance  $t(d)$  are obtained by applying multilayer optics.<sup>31</sup> The application of multilayer optics is necessary because the film thickness is on the same order as the mean absorption depth  $\alpha^{-1}$  of bismuth (cf. Table I). As Si has an order of magnitude larger mean adsorption depth than bismuth, the Bi/Si heterosystem can be treated as a thin absorbing film on a nonabsorbing substrate. By using the optical constants for Bi and Si listed in Table I, the resulting absorptance  $\eta(d)$  versus film thickness is shown in Fig. 3(c). With increasing film thickness,  $\eta(d)$  increases and reaches the bulk value of 0.34 for  $d \gg \alpha^{-1}$  (not shown here;  $r=0.66$  and  $t=0$ , cf. Table I).

For the 11 nm thin film shown in Fig. 3(a),  $\eta=0.18$  and Eq. (5) yields a slope of  $\Delta T/Q_A=137.5 \text{ K}/(\text{mJ}/\text{cm}^2)$ . This is more than three times the observed value and significantly larger than the experimental error. In Fig. 3(b), the result of Eq. (5) using  $\eta(d)$  from Fig. 3(c), multiplied by a factor of 1/4, is displayed as a solid line. Besides the magnitude of  $\Delta T/Q_A$  calculated by the above simple model, the general trend shows a decreasing slope with increasing film thickness, which is not observed in the experiment. The experimentally observed thickness-independent  $\Delta T/Q_A$  can be explained if the absorbed energy is not homogeneously distributed across the film as assumed in the simple model. On the contrary, an inhomogeneous temperature distribution across the film is only expected for delays below 10 ps.<sup>7</sup> For larger time delays, heat diffusion in the film leads to a homogeneous temperature distribution. Another possible explanation are thickness dependent material parameters, i.e., specific heat  $c$  and complex index of refraction  $\tilde{n}=n+i\kappa$ , which are taken as bulk values in the above model.

More striking is the large difference of about a factor of 4 between the observed and expected magnitude of the slope  $\Delta T/Q_A$ . This difference can again be attributed to the modified material constants of thin Bi films compared to the bulk values. Additionally, it was found for Bi bulk that the reflectivity for photons of wavelength 800 nm is temperature dependent and increases from 0.66 at 300 K to 0.9 at 80 K.<sup>32</sup> Because the optical constants are only known for 300 K, the

calculation of the absorptance  $\eta(d)$  uses the optical parameters for a sample temperature of 300 K. With respect to the reflectivity change with increasing temperature, this yields an upper limit of the slope  $\Delta T/Q_A$ . In principle, internal reflection effects, i.e., the dynamic change of the reflectivity during excitation, has to be considered, too.<sup>33</sup> However, even if the reflectivity is as low as for 80 K throughout the excitation, the difference of the experimental and expected slope  $\Delta T/Q_A$  cannot be explained.

We conclude that the initial surface temperature rise is caused by linear absorption, but the magnitude of the initial temperature rise is a factor of 4 smaller than expected. A satisfying explanation for this difference cannot be given unless the thickness dependence of the material constants is known.

## DECAY CONSTANT $\tau_2$

The dependence of the decay constant  $\tau_2$  on the applied fluence  $Q_A$  and film thickness  $d$  is shown in Fig. 4. As is evident from Fig. 4(a), the decay constant is independent of the fluence. For an 11 nm thin Bi film, the average value yields  $\tau_2=(1350 \pm 160)$  ps with a standard deviation as error. From the decay constant, the thermal boundary conductance can be obtained by applying Eq. (2) and  $c$  from Table I, yielding  $\sigma_K=(970 \pm 115) \text{ W}/(\text{cm}^2 \text{ K})$ , which is in accordance with the previously determined value.<sup>22,23</sup>

As obvious from Eq. (3),  $\tau_2$  can only be independent of the applied fluence and, thus, the initial temperature jump (cf. Fig. 3) if  $\langle v_z \rangle \cdot \langle t \rangle$  is temperature independent. Note that any temperature dependence of the decay constant introduced by  $\sigma_K$  is canceled out [cf. Eq. (2)] because  $\sigma_K \propto c(\omega, T)$ . In addition,  $\sigma_K$  was found to be constant in our investigated temperature range.<sup>37</sup>

Figure 4(b) shows the dependence of the decay constant  $\tau_2$  on the film thickness  $d$ . In the thickness range from 6 to 12.2 nm,  $\tau_2$  linearly depends on  $d$ , which is expected from Eq. (2). A line fit yields a slope of  $(90 \pm 4)$  ps/nm. By using  $c$  from Table I, this results in a thermal boundary conductance of  $\sigma_K=(1320 \pm 60) \text{ W}/(\text{cm}^2 \text{ K})$ , which is somewhat larger than the above determined value. The origin of this difference is not clear, but the value determined from the slope is more reliable because it is derived from a series of measurements.

The value for the thermal boundary conductance derived from the thickness dependence is in good agreement with the value calculated from the use of the acoustic mismatch model for the phonon transmission probability.<sup>22,23</sup> Recently, the thermal boundary conductance of the epitaxial Bi-Si interface was predicted to be a factor of 2 smaller than what we observed.<sup>37</sup> However, mode conversion was not included in the derivation of the thermal boundary conductance, i.e., longitudinally polarized phonons in Bi only scatter into longitudinally polarized phonons in Si.<sup>37</sup> Our results suggest that for the Bi-Si interface, mode conversion has to be included, which increases the transmission probability. This supports the previous results of the phonon transmission calculations in the scope of the acoustic mismatch model, where it was found that the longitudinal to transversal polarized phonon

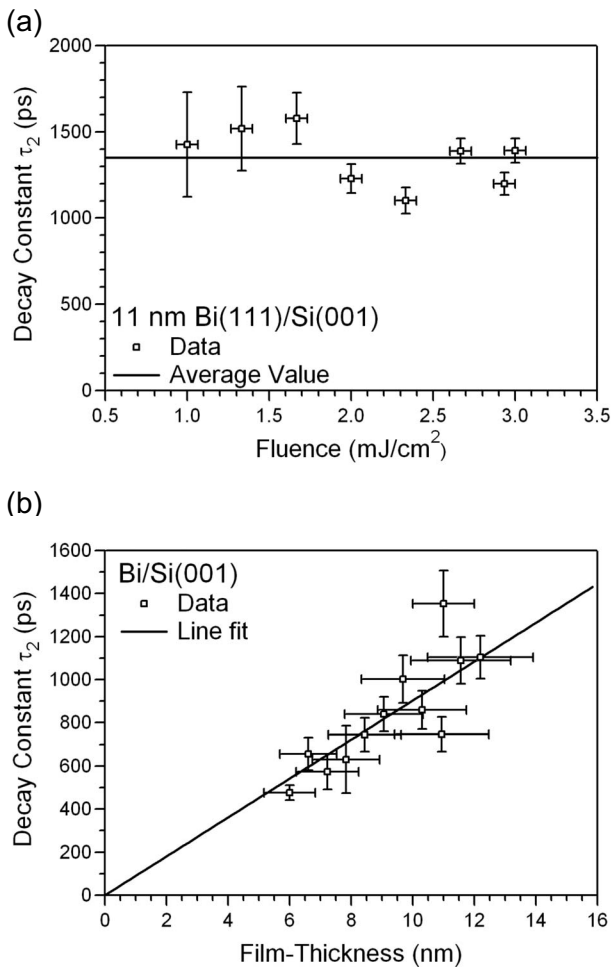


FIG. 4. Dependence of the decay constant  $\tau_2$  on (a) the fluence  $Q_A$  and (b) the film thickness  $d$ . In (a), the average value for an 11 nm thin Bi film yields  $(1350 \pm 160)$  ps, with a standard deviation as error (solid line). The dependence of  $\tau_2$  on the film thickness shown in (b) is described by a linear relationship with a slope of  $(90 \pm 4)$  ps/nm (solid line). By applying Eq. (2), and  $c$  from Table I, this yields a thermal boundary conductance of  $\sigma_K = (1320 \pm 60)$  W/(cm<sup>2</sup> K).

conversion is the dominant contribution to the heat transport across the interface.<sup>23</sup>

Along the above discussion for the fluence dependence, any thickness dependence of  $\sigma_K$  is cancelled out for the de-

decay constant [cf. Eq. (2)]. From the linear behavior of  $\tau_2$ , it can be concluded that in the investigated thickness range,  $\langle v_z \rangle \cdot \langle t \rangle$  is independent of the film thickness. Two different possibilities can explain this observation. First, the thin films already have bulk properties that are used for the derivation of the phonon transmission probability across the interface. Second, the phonon transmission probability is not determined by bulk properties, but by the properties of the interface itself. From the above data, one or the other possibility cannot be ruled out. However, with decreasing film thickness, the properties of the bulk, i.e., phonon dispersion and density of states, will eventually be altered because of the finite size in one direction. If the transmission probability is given by bulk properties, this will result in a deviation from the linear relationship between the decay constant and the film thickness. On the contrary, if the heat transport across the interface is given by the interface itself, this linear relationship will hold, as the interface properties are independent of the bulk properties. Future experiments with ultrathin films are planned, which will shed light on this issue of the heat transport across the interface.

## SUMMARY

We have presented the results on the thermal response of epitaxial Bi films on a Si substrate to femtosecond laser pulse excitation. It was shown that the initial temperature increase of the film can be explained by linear absorption. The surface cooling follows an exponential behavior, which is determined by the thermal boundary conductance. The time constant of the decay linearly depends on the film thickness in the range from 6 to 12.2 nm. The thermal boundary conductance extracted from this linear relationship is  $\sigma_K = (1320 \pm 60)$  W/(cm<sup>2</sup> K), which is in good agreement to the calculated value using the acoustic mismatch model for the determination of the phonon transmission probability.

## ACKNOWLEDGMENTS

The authors thank T. Payer for the AFM investigation; C. Deiter, J. Weissenmüller, and J. Wollschläger for the x-ray reflectometry measurements; and P. Zhou for technical support. This work is funded by the Deutsche Forschungsgemeinschaft through SFB 616 “Energy dissipation at surfaces.”

\*boris.krenzer@uni-due.de

<sup>1</sup>C.-W. Nan, R. Birringer, D. R. Clarke, and H. Gleiter, *J. Appl. Phys.* **81**, 6692 (1997).

<sup>2</sup>D. G. Cahill, W. K. Ford, K. E. Goodson, G. D. Mahan, A. Majumdar, H. J. Maris, R. Merlin, and S. R. Phillpot, *J. Appl. Phys.* **93**, 793 (2003).

<sup>3</sup>E. T. Swartz and R. O. Pohl, *Rev. Mod. Phys.* **61**, 605 (1989).

<sup>4</sup>R. J. Stoner and H. J. Maris, *Phys. Rev. B* **48**, 16373 (1993).

<sup>5</sup>C. Chiritescu, D. G. Cahill, N. Nguyen, D. Johnson, A. Bodapati,

P. Koblinski, and P. Zschack, *Science* **315**, 351 (2007).

<sup>6</sup>R. M. Costescu, D. G. Cahill, F. H. Fabreguette, Z. A. Sechrist, and S. M. George, *Science* **303**, 989 (2004).

<sup>7</sup>B. Krenzer, A. Hanisch, A. Duvenbeck, B. Rethfeld, and M. Horn-von Hoegen, *J. Nanomaterials* (to be published 2008).

<sup>8</sup>D. A. Young and H. J. Maris, *Phys. Rev. B* **40**, 3685 (1989).

<sup>9</sup>P. E. Phelan, *J. Heat Transfer* **120**, 37 (1998).

<sup>10</sup>P. Reddy, K. Castelino, and A. Majumdar, *Appl. Phys. Lett.* **87**, 211908 (2005).

- <sup>11</sup>G. Chen, Phys. Rev. B **57**, 14958 (1998).
- <sup>12</sup>L. De Bellis, P. E. Phelan, and R. S. Prasher, J. Thermophys. Heat Transfer **14**, 144 (2000).
- <sup>13</sup>R. S. Prasher and P. E. Phelan, J. Heat Transfer **123**, 105 (2001).
- <sup>14</sup>G. Fagas, A. G. Kozorezov, C. J. Lambert, and J. K. Wigmore, Physica B **263-264**, 739 (1999).
- <sup>15</sup>A. Majumdar and P. Reddy, Appl. Phys. Lett. **84**, 4768 (2004).
- <sup>16</sup>J. Miklowitz, *The Theory of Elastic Waves and Waveguides*, Applied Mathematics and Mechanics Vol. 22 (North-Holland, Amsterdam, 1978).
- <sup>17</sup>H.-K. Lyeo and D. G. Cahill, Phys. Rev. B **73**, 144301 (2006).
- <sup>18</sup>G. Jnawali, H. Hattab, F. J. Meyer zu Heringdorf, B. Krenzer, and M. Horn-von Hoegen, Phys. Rev. B **76**, 035337 (2007).
- <sup>19</sup>G. Jnawali, H. Hattab, B. Krenzer, and M. Horn-von Hoegen, Phys. Rev. B **74**, 195340 (2006).
- <sup>20</sup>H. Hattab, E. Zubkov, A. Bernhart, G. Jnawali, C. Bobisch, B. Krenzer, M. Acet, R. Möller, and M. Horn-von Hoegen, Thin Solid Films (to be published 2008).
- <sup>21</sup>T. Nagao, S. Yaginuma, M. Saito, T. Kogure, J. T. Sadowski, T. Ohno, S. Hasegawa, and T. Sakurai, Surf. Sci. **590**, L247 (2005).
- <sup>22</sup>A. Janzen, B. Krenzer, P. Zhou, D. von der Linde, and M. Horn-von Hoegen, Surf. Sci. **600**, 4094 (2006).
- <sup>23</sup>B. Krenzer, A. Janzen, P. Zhou, D. von der Linde, and M. Horn-von Hoegen, New J. Phys. **8**, 190 (2006).
- <sup>24</sup>P. Kury, R. Hild, D. Thien, H.-L. Günter, F.-J. Meyer zu Heringdorf, and M. Horn-von Hoegen, Rev. Sci. Instrum. **76**, 083906 (2005).
- <sup>25</sup>E. A. Murphy, H. E. Elsayed-Ali, and J. W. Herman, Phys. Rev. B **48**, 4921 (1993).
- <sup>26</sup>A. Janzen, B. Krenzer, O. Heinz, P. Zhou, D. Thien, A. Hanisch, F.-J. Meyer zu Heringdorf, D. von der Linde, and M. Horn-von Hoegen, Rev. Sci. Instrum. **78**, 013906 (2007).
- <sup>27</sup>C. Kittel, *Introduction to Solid State Physics*, 12th ed. (Oldenbourg, Munich, 1999).
- <sup>28</sup>C.-K. Sun, F. Vallée, L. Acioli, E. P. Ippen, and J. G. Fujimoto, Phys. Rev. B **48**, 12365 (1993).
- <sup>29</sup>L. Guidoni, E. Beaurepaire, and J.-Y. Bigot, Phys. Rev. Lett. **89**, 017401 (2002).
- <sup>30</sup>K. Sokolowski-Tinten *et al.*, Nature (London) **422**, 287 (2003).
- <sup>31</sup>F. Abelès, *Optics of Thin Films*, Advanced Optical Techniques (North-Holland, Amsterdam, 1967).
- <sup>32</sup>M. Cardona and D. L. Greenaway, Phys. Rev. **133**, A1685 (1964).
- <sup>33</sup>G. Chen and C. L. Tien, J. Appl. Phys. **73**, 3461 (1993).
- <sup>34</sup>Landolt-Börnstein, *Condensed Matter*, New Series, Group III, Vol. 15, Pt. C (Springer, New York, 2005).
- <sup>35</sup>D. E. Aspnes and A. A. Studna, Phys. Rev. B **27**, 985 (1983).
- <sup>36</sup>J. B. Renucci, W. Richter, M. Cardona, and E. Schön herr, Phys. Status Solidi B **60**, 299 (1973).
- <sup>37</sup>J. Wang and J.-S. Wang, J. Phys.: Condens. Matter **19**, 236211 (2007).